Range-based 3D Mapping Aided GNSS with NLOS Correction based on Skyplot with Building Boundaries

Hoi-Fung Ng, Guohao Zhang and Li-Ta Hsu

Interdisciplinary Division of Aeronautical and Aviation Engineering, The Hong Kong Polytechnic University

BIOGRAPHY (IES)

Mr Hoi-Fung Ng received the Bachelor of Engineering (Honours) in Air Transport Engineering from the Interdisciplinary Division of Aeronautical and Aviation Engineering, He is currently a research assistant in the same department. The Hong Kong Polytechnic University, Hong Kong, in 2018. His research interests include the 3D mapping-aided GNSS localization, navigation.

Mr. Guohao Zhang received the bachelor degree in Mechanical Engineering and Automation from University of Science and Technology Beijing, China, in 2015. He received the master degree in Mechanical Engineering and currently is PhD student in the Hong Kong Polytechnic University. His research interests including GNSS urban localization, vehicle-to-vehicle cooperative localization and multi-sensor integrated navigation.

Dr Li-Ta Hsu is an Assistant Professor in the Division of Aeronautical and Aviation Engineering at Hong Kong Polytechnic University. Dr Hsu has been member of Editorial Board in GPS Solutions since 2015. He is an Associate Fellow of RIN. From 2014 to 2016, he was a postdoctoral researcher at the University of Tokyo, after his stay in Tokyo Marine University as visiting researcher. From 2012 to 2013, he was a visiting researcher in University College London. He received BSc and PhD degree in Aeronautics and Astronautics from National Cheng Kung University, Taiwan, in 2007 and 2013, respectively. His technical expertise and interests include the detection, mitigation and correction of GNSS multipath and NLOS effects to improve GNSS positioning performance in the super-urbanized cities using 3D Mapping Aided GNSS, 3D LiDAR Aided GNSS and Vector Tracking approaches.

ABSTRACT

The performance of conventional global navigation satellite system (GNSS) positioning in dense urban area is still a challenge due to the signal reflecting by building and result in multipath and non-light-of-sight (NLOS) receptions. These effects are much affecting the low-cost GNSS receiver (e.g. smartphone). A novel range-based 3D mapping aided (3DMA) GNSS with NLOS correction based on skyplot with building boundaries is proposed in this paper. Instead of using ray-tracing simulation, we propose to detect the reflection points from the skyplot with building boundaries. With the assumption that reflected signals

https://doi.org/10.33012/2019.16774

follow the rule of reflection, the reflected points are only possible located at certain points on the skyplot. After the possible reflection being found, we can obtain the reflecting delay distance of NLOS reception for each candidate based on its distance between the reflecting point. Then, the pseudorange for each signal can be simulated based on the geodetic distance between candidate and other error term (e.g. satellite clock offset, ionosphere and tropospheric delays, etc.). Afterward, a set of simulated pseudorange will compare to the measurements and giving a score to the corresponding candidate. Finally, the user position is determined by averaging the position of candidates with score weighting, indicates the position with a simulated pseudorange most matching to the measurements. The proposed algorithm is verified through real experiments in the dense urban areas in Hong Kong. A commercial grade GNSS receiver is employed to collect the raw data. The performance of the proposed algorithm is compared with the conventional weighted least square (WLS) and the ray-tracing based 3MDA GNSS. According to the results, the proposed algorithm is able to correctly simulate the pseudorange error with lower computation load and further achieves positioning accuracy with less than 10 meters error.

1. INTRODUCTION

Accurate positioning is essential for smartphone users. The positioning solution of the smartphone is mainly determined by a low-cost built-in global navigation satellite system (GNSS) receiver. With current assisted global positioning system (AGPS) technology, the smartphone can achieve positioning solution within a few meters of error in open areas. However, the urban area is still a challenging environment with the majority of smartphones, usually suffering dozens of meter positioning error. In the urban area, the GNSS signal can be blocked by the buildings or reflected by the building surface. Hence, both the direct and reflected signals or only the reflected signals are being received, namely the multipath and non-light-of-sight (NLOS) reception respectively. The extra traveling distance of the reflected signal can further introduce enormous error during positioning, as the major error source of GNSS urban positioning [1].

To improve the urban positioning accuracy, different researches focused on the exclusion of NLOS affected measurement. For example, they are using the consistency-check method which is similar to receiver autonomous integrity monitoring (RAIM) [2] to exclude the unhealthy range-measurements，achieving a satisfactory positioning result. However, it is not effective for the dense urban scenario with severe NLOS reception. Too much NLOS receptions as the outliers may lead to incorrect unhealthy satellite classification [3]. Other researches also proposed to use the dual-polarization antenna to distinguish the NLOS signals from measurements [4]. This approach requires special antenna, which is usually complex with large size and not feasible for smartphones. Another approach is similar to 3DMA GNSS, by using the 3D light detection and ranging (LiDAR), the NLOS signals are able to be detected [5] and corrected based on scanned surrounding building distance and NLOS propagation model [5]. This method also requires extra equipment and power consumption which are not practical for a hand-held device. There is also a method using the fisheye camera to detect the NLOS signal by image recognition and determine the satellites visibility [6, 7]. It does not need extra equipment but need the camera turning on for a long period while positioning, which also impractical for a smartphone.

To prevent adding extra equipment and make use of all the received measurements, the 3DMA GNSS positioning algorithms as shadow matching [8, 9] and ray-tracing [10, 11], were proposed to improve the positioning in dense urban areas. For the shadow matching, the building boundaries known by the 3D building model and the satellites positions by the ephemeris data, are

projected on the skyplot so that the positioning result can be obtained from the scoring scheme by the visibility of satellites from several locations. It can improve the across-street positioning accuracy effectively, however, not in the along-street direction due to the similarity of building geometry on along-street direction [12]. Due to the insufficient direction of shadow matching, a ray-tracing based 3DMA GNSS positioning algorithms were developed to detect and correct the reflected signal on NLOS and multipath propagation. This method traces the possible transmission route of both direct and reflected GNSS signals based on 3D building models. Hence, the pseudorange error can be simulated and further corrected to improve the positioning accuracy. This approach can provide a precise pseudorange error correction in the pseudorange level measurement and provide a positioning accuracy about 10m or lower [10]. With correction on NLOS signals, the NLOS measurements become useful for positioning, which gives a better dilution of precision (DOP) and sufficient measurement amount even in dense urban areas. However, it requires a high computation load as the ray-tracing positioning is based on the comparison between simulated pseudorange and the measurements [13]. These criteria lead to a high-performance computing platform to apply the ray-tracing algorithm, which is not feasible real-time positioning by a smartphone. As a result, to perform an accurate positioning as the ray-tracing method without extensive computation load is desired.For the ray-tracing approach, numbers of the candidate are firstly distributed around. Then, each candidate needs to simulate the transmission path of each signal on every building surface. These simulations are computationally expansive. Furthermore, the positioning performance also depends on the level of detail (LOD) of the 3D building model, and the consideration of multiple reflections. The more detail on the 3D model and consider multiple signal reflection, the more realistic path can be obtained with precise pseudorange correction. Meanwhile, the computation load is also raised for operation. With the above limitation, this paper proposes to replace the ray-tracing algorithm. To estimate the NLOS delay in pseudorange domain, we propose to use the characteristic of reflection, where the incidence angle is identical with the reflection angle for a perfect reflection. The elevations are equal, and the azimuths are symmetric regarding the building distribution for the satellite and the corresponding reflecting point. Therefore, innovatively, based on the surrounding building boundary projected on the skyplot and the satellites position, the possible reflecting point of signals can be directly observed. This assumption makes use of the characteristic of NLOS transportation, avoids searching the appropriate reflection point on each building surface, which significantly decreases the computation requirements. This simplification still maintains the performance of reflected signal simulation as well as the accuracy of NLOS correction with regarding the conventional approach. In a word, the proposed simplified ray tracing NLOS correction algorithm is applicable for smartphone achieving real-time accurate positioning solution in dense urban with the presence of many unhealthy measurements.

2. OVERVIEW OF THE PROPOSED 3DMA GNSS ALGORITHM

Figure 1 shows the flowchart of the proposed algorithm. The algorithm can be divided into two main parts; offline and online processes.

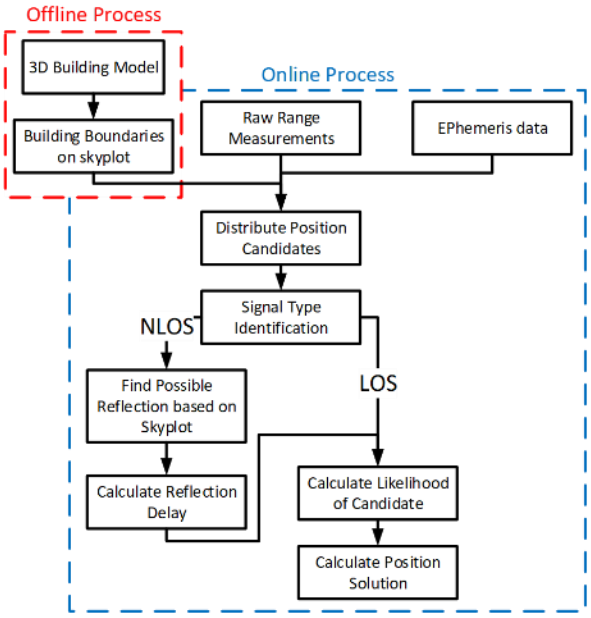

Figure 1 - Flowchart of the proposed range-based 3DMA GNSS algorithm

The offline processes are to generate the building boundaries on skyplot, and it is called 'skymask' in this paper. This part is the most required computation power. Hence these processes are done offline to reduce computation load for the receiver. The skymask are stored in a specific format and save inside the receiver, which will be retrieved afterward.

In the online positioning stage at each epoch, position candidates are distributed evenly around the initial position after receiver acquired the measurements. In each candidate, the satellites' position in Earth-Centered, Earth-Fixed (ECEF) is converted into local coordinate (azimuth, elevation) and placed on the skyplot. Therefore, based on the satellite position and corresponding building boundaries 'shadow', satellites can be identified to the type of LOS and NLOS signals. As well as for the NLOS labeled measurement, based on the polar information, and apply the law of reflection, the possible reflecting point. Therefore, the reflection delay can be found and correct the NLOS signal. After that, if the type of measurement is agreed by both skymask labeling and measurement signal strength, it is selected as the valid satellite measurement for the candidate. The simulated pseudorange is calculated for each valid satellite on each candidate. Them, we compare the similarity between measured and simulated pseudorange. A scoring scheme based on the average of pseudorange difference on each candidate is applied to score each candidate. A smaller difference will be given a higher score. Finally, the weighted 2D position solution is calculated, and the height is corrected by the geodetic datum at the last since a land application is assumed.

3. ALGORITHMS

3.1. Skymask Generation

In the offline stage, the building boundaries are projected on the skyplot, also named 'skymask'. The skymask is a polar plot constructed by azimuth and elevation angle. It represents the building edge location in angle information on a particular location. If the satellite placed on a lower elevation than the building boundary elevation (under the same azimuth angle), the satellite signal is suggested to be blocked by the building which is also known as NLOS signal.

The skymask of each location is generated with the 3D city model offline. Thus, the skyplot with building boundaries can be initially stored in the smartphone or requested from the server. Based on the 3D building model or in storage perspective, a specific area is selected out and divided into grid points to construct the skymask table, in here the grid point separation is 2m to generate the skymask. The example of the generated skymask is saved as the following format.

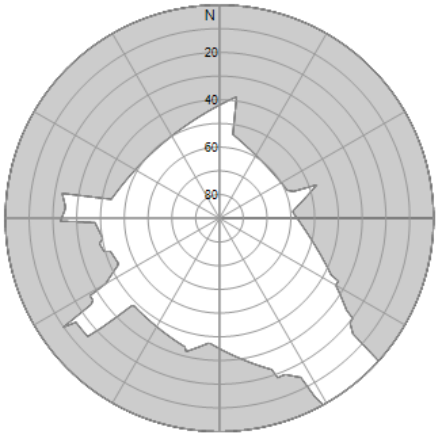

Azimuth (degree)	Elevation (degree)
1	41.8
2	41.3
3	40.9
⋮	⋮
359	42.7
360	42.3

Figure 2 - Example of skymask (left) and skymask array (right)

In each location, it will be divided into outside building and inside the building. For the outside building location, an azimuth angle list of total 360-degree will be used to store the maximum elevation angle of building edge for corresponding azimuth angle, as shown in Figure 2; for the inside building location, a flag with a negative value of building height will be used to present a specific location is a building. For example, the cell obtains value '-58' represent this location is inside building, and this building tall 58m.

This offline generation perspective is especially important for a low-cost device with limited computational power. Device with low computational power is nearly impossible to generate the skymask every time neither in time consumption nor power management aspect. This step is similar to the process that the study proposed in [8], but this paper also includes the building height information for the later use on the NLOS correction.

3.2. NLOS Correction based on the Generated Skymask

In the real-time positioning; First, an initial position is given by standard point positioning (SPP) at each epoch to distribute positioning candidates around, here the weighted-least-square (WLS) [14] will be used. By a grid of area 50m x 50m with 2m separation between adjacent candidates will be constructed. Distributing the particles in grid is more efficient than in Gaussian distribution [15]. If the candidate is distributed inside the building, it will not be valid to calculate its likelihood. Then on the candidates' level, the satellites are projected on the skyplot of each candidate based on their position with ephemeris data, as well as loading the corresponding building mask on the skyplot. As a result, the satellites are identified as the type of LOS and NLOS from the building skymask on each candidate.

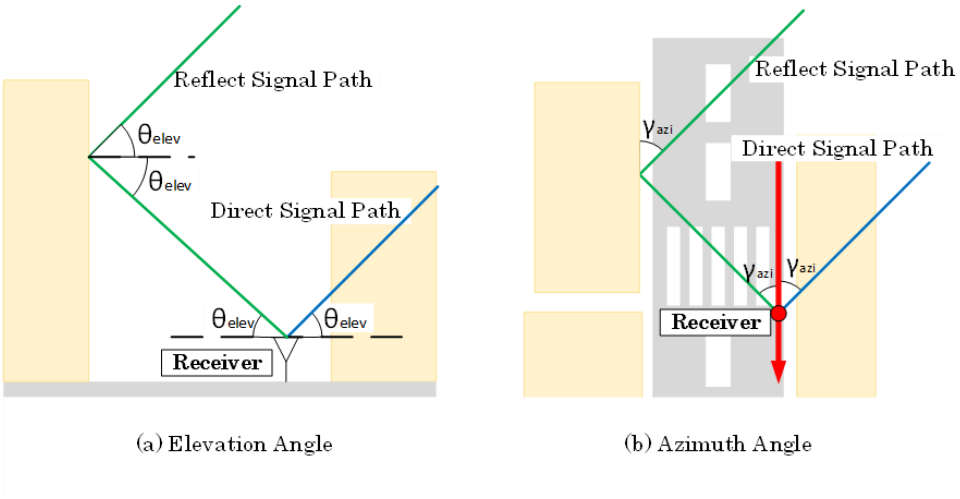

Figure 3 - Demonstrate on the angular relationship on elevation angle (left) and azimuth angle (right)

As indicated in [1], an NLOS delay can be modeled based on elevation angle and lateral distance from the receiver to the reflector. As shown in Figure 3(a), the elevation angle of the direct signal path and reflect signal path are the same if the law of reflection is assumed (i.e., we assumed all building surfaces are smooth and perfect reflection can be occurred).

For the azimuth angle, the angle between the satellite and align axis is the same as the angle between the reflecting point and align axis, shown in Figure 3(b). As a result, we can find the azimuth and elevation angles of the reflecting point for the NLOS identified satellites on each candidate.

For the azimuth and elevation angles, we can assume the blocked direct single and the first part of the reflected signal (from satellite to reflecting point) are parallel since the distance between the satellite to ground is relatively far away. Therefore, the azimuth angle between the wall surface and the satellite is the same as the align axis and the satellite; the elevation angle between the normal of the wall and the satellite is the same as the ground and the satellite.

In here, the geometry meaning of the align axis is the parallel direction of the building surface that the reflection occurs. Therefore, the azimuth angle between the satellite and the axis is as same as the angle between the reflecting point and the axis, as shown in Figure 4. For the implementation in this paper, the direction of the axis is inputted manually first. Furthermore, for the street that all buildings' parallel direction are the same, we can assume the align axis direction is a fixed value for the area like in Figure 7(a).

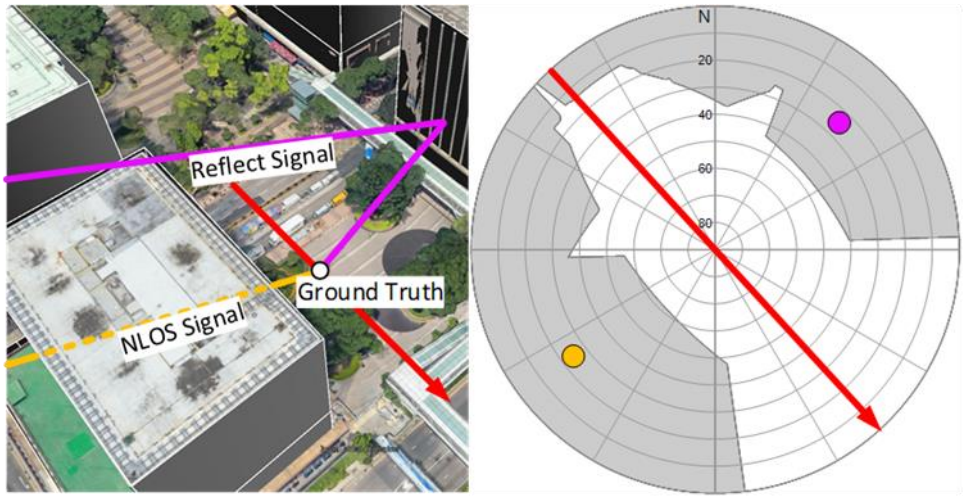

Figure 4 - Actual position (left) and their polar position projected on skymask (right)

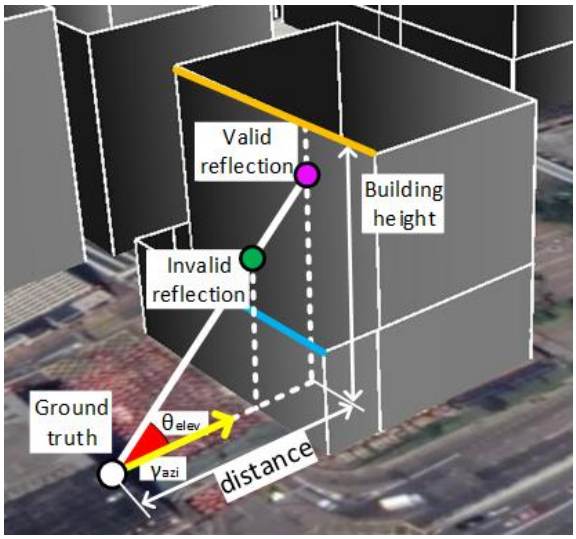

Figure 5 - Example on finding the valid reflecting point

After we known azimuth angle, we can find the building location on the skymask table along corresponding azimuth angle of reflecting point. For example in Figure 5, from the distance between building and candidate location as well as building height, the elevation angle of the top of the building can be calculated. If the calculated building height elevation angle is smaller than the elevation angle of reflecting point on sky plot, means the reflecting point is not falling on this shadow building area (like the green point in Figure 5). Then it will keep looking for the next building and repeat finding the nearest building along azimuth angle until found the calculated building height elevation angle is larger than that of reflecting point on sky plot, which the reflecting point falls on the corresponding building (the purple point in Figure 5). As a result, the coordinate of reflecting point can be obtained, as well as the reflection delay, $\varepsilon_n^{refl(i)}$.

$$
\begin{aligned}
&Refelciton\ delay\ \varepsilon_n^{refl(i)} \\
&\quad = Reflect\ path_{satellite\ to\ reflect\ point} \\
&\quad + Reflect\ path_{reflect\ point\ to\ position\ candidate} - Direct\ NLOS\ path
\end{aligned} \tag{1}
$$

3.3. Simulated Range Calculation

After that, to evaluate the likelihood of the position candidates, the similarities between the pseudorange measurement $\tilde{\rho}$ and simulated range $\hat{\rho}$ on each position candidate are required. The simulated range $\hat{\rho}_n^i$ between the n-th satellite, x_n^{sv}, and the i-th position candidate, P^i, can be calculated by the sum of the geometric distance $R_n^i = \|x_n^{sv} - P^i\|$, correction for satellite clock, $c\delta t_n^{sv}$, ionosphere errors (using the Klobuchar model), I_n, and troposphere errors, T_n and the reflection delay distance, $\varepsilon_n^{refl(i)}$ found in above step if applicable, as following,

$$
\hat{\rho}_n^i = R_n^i + c\delta t_n^{sv} + I_n + T_n + \varepsilon_n^{refl(i)} \tag{2}
$$

To eliminate the receiver clock offset, a reference satellite will be selected and all measured pseudorange, as well as simulated range, are differenced once to obtain the single difference (SD) of the ranges on each candidate. The reference satellite $r(n)$ is selected by the satellite with the highest elevation angle for each constellation.

$$
D_n^i = \left|\left(\tilde{\rho}_n^i - \tilde{\rho}_{r(n)}^i\right) - \left(\hat{\rho}_n^i - \hat{\rho}_{r(n)}^i\right)\right| \tag{3}
$$

And the likelihood of each candidate is calculated by the average of differenced SD ranges. Table 1 shows the rule of signal type classification, where the measurement can be classified into LOS and NLOS by the received signal strength classification and the proposed method based on position candidates classification with skymask. If and only if the signal type agrees between the proposed method and signal strength classification, the satellite is used to calculate the likelihood for this candidate. Furthermore, if the reference satellite is the only satellite that agrees on signal type, the corresponding candidate will not be scored, and a large value is set to the likelihood.

$$
\propto^i = {N_{sim}}^{-1} \times \sum_n^{N_{sim}} D_n^i \tag{4}
$$

Table 1 - Rule of signal classification based on the received signal strength and the proposed method

		Proposed method			
		LOS	Multipath	NLOS, no reflect path found	NLOS, reflect path found
Signal Strength Classification	> 35 dB Hz (LOS)	Valid	Valid	Invalid	Invalid

	< 35 dB Hz (NLOS)	Invalid	Invalid	Invalid	Valid

The likelihood will then perform a rescaling between 0 to 1 and be the score of the candidates. A smaller value of the likelihood, the higher score is. In other words, it means the simulated range is more matching with the measurement.

$$\propto^{i\prime} = \frac{\max(\propto) - \propto^{i}}{\max(\propto) - \min(\propto)} \tag{5}$$

Then all the valid candidates are z-normalized.

$$\Lambda^{i} = \frac{\propto^{i\prime} - \overline{\propto^{i\prime}}}{\sigma} \tag{6}$$

The final step is to determine the range-based 3DMA with NLOS correction with skymask position solution. The top 5% candidates with highest scored are selected to calculate the weighted average position.

$$x(t) = \frac{\sum_i \Lambda^{i}(t) P^{i}(t)}{\sum_i \Lambda^{i}(t)} \tag{7}$$

As a result, a 2D-coordinate can be obtained (latitude, longitude), and here an assumption is made, the device always stays to the ground (mean sea level). Therefore, the height of the calculated position is then corrected by the mean sea level datum [16] provided by The Geodetic Survey Section of Survey and Mapping Office (SMO) of the Lands Department.

4. EXPERIMENTS RESULTS

To evaluate the performance of the proposed algorithm, a commercial grade GNSS receiver (u-blox M8T) is used to record raw measurements in the dense urban areas in Hong Kong. The antenna used in the experiment is the u-blox ANN-MS antenna, namely a patch antenna. The output rate of the u-blox receiver is set to 1 Hz. The constellations on GPS and BeiDou are enabled.

Figure 6 - U-Blox M8T setup

The NLOS correction with skymask is comparing with the ray-tracing positioning algorithm [11]. The ray-tracing algorithm only considers single reflection for signal, and only provide reflection delay correction for those reflect path found NLOS signals. The difference between the two algorithms is only the NLOS correction is providing by the skymask based algorithm. Therefore, we can evaluate the reflection correction provided by skymask NLOS correction method compare with ray-tracing.

Several experiments were taken in Hong Kong dense urban to evaluate the performance of our proposed method and compared with ray-tracing positioning algorithm. Two situations were simulated when performing the pro-processing. First is the 'ideal case', the positioning candidates were distributed based on ground truth for every epoch, and the signal classification is using the result on ground truth, which means all signal are classified correctly; while the other is the 'real case', the positioning candidates were distributed around the weighted-least-square, and classify the signals with signal strength to perform an actual SSP situation when normal use. The evaluation of position solution can be divided into 2D, along, and across direction. The 2D error represents the total east and north displacement away from ground truth. The along street error represents the error distance of direction that parallel to the skymask's align axis direction; while the across street error is the error distance of direction that perpendicular to the guiding axis.

The experiment results are post-processed by quad-core i7 7th generation CPU. The proposed method takes about 16-second for one epoch result while the ray-tracing takes about 2.5-minute for epoch positioning. Which the skymask correction is about 10 times faster than ray-tracing in single epoch positioning.

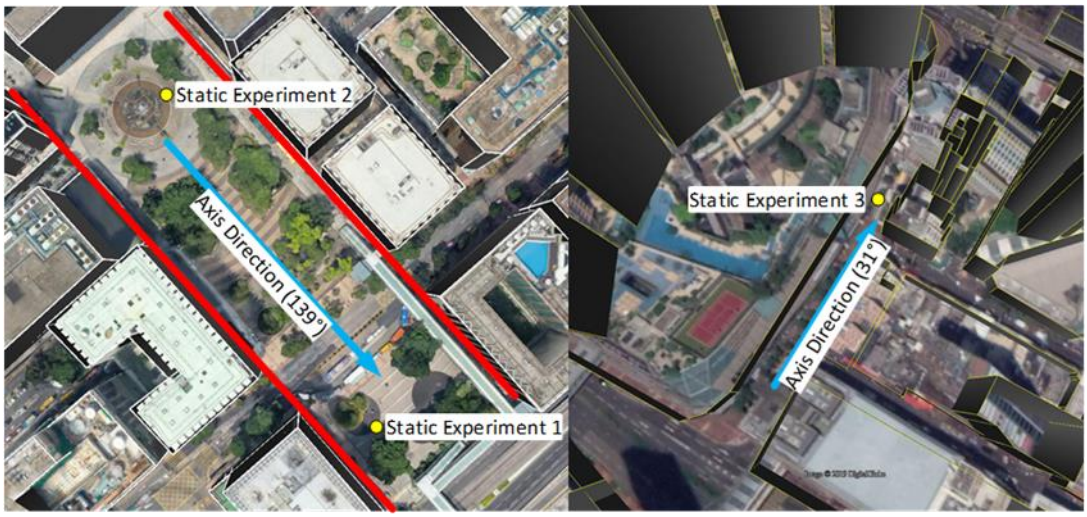

Figure 7 - Static experiments take places in Tsim Sha Tsui East (left) and Tsuen Wan West (right)

Two static experiments were taken in the Tsim Sha Tsui East, Hong Kong, shown in Figure 7(a). Both two experiments conducted 2 minutes (120 epochs). The first static experiment placed in a more 'tidy' environment, which the buildings near are aligned. Therefore, the signals are most likely to be reflected above these two buildings' surface.

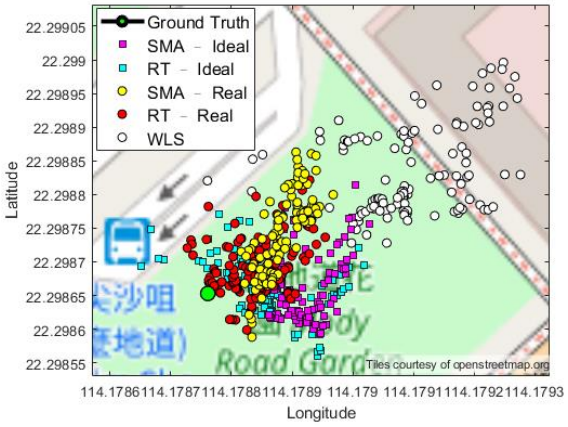

Figure 8 - Static experiment 1 results

Table 2 - Static experiment 1 (SMA: skymask axis method, RT: ray-tracing, WLS: weighted least square)

	2D-Error (m)		Along-Street Error (m)		Across-Street Error (m)	
	Mean	S.D.	Mean	S.D.	Mean	S.D.
SMA – Ideal	16.66	4.73	9.41	4.43	12.86	5.18
RT – Ideal	11.92	5.82	7.71	5.06	8.37	4.57
SMA – Real	15.87	6.04	3.16	2.06	15.18	6.61

RT – Real	10.51	5.62	3.74	2.63	9.25	5.80
WLS	41.25	10.21	9.03	4.85	39.91	10.41

From the results of static experiment 1 in Table 2 and Figure 8, the mean error of the skymask axis method of the ideal and real case are 16.66m and 15.87m respectively, compared to the ray-tracing algorithm of mean error are 11.92m and 10.51m. The error is about 30% more compare to the ray-tracing.

The second static experiment took place in a deeper urban with three side buildings, two sides are parallel to the align axis while one side (red surface in Figure 10(a)) is perpendicular to the guiding axis, which means some signal may reflect over the perpendicular surface and result in misdetection a wrong reflecting point for NLOS correction.

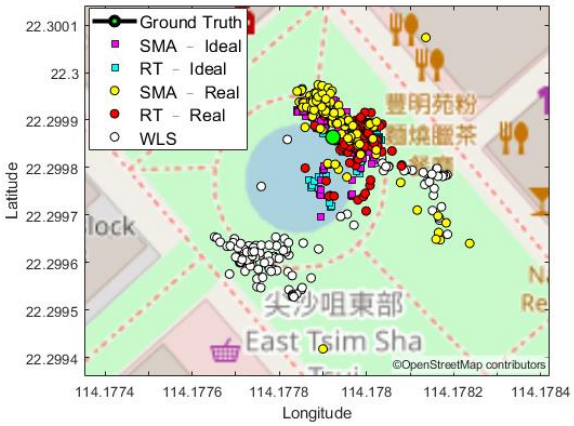

Figure 9 - Static experiment 2 results

Table 3 - Static experiment 2 (SMA: skymask axis method, RT: ray-tracing, WLS: weighted least square)

	2D-Error (m)		Along-Street Error (m)		Across-Street Error (m)	
	Mean	S.D.	Mean	S.D.	Mean	S.D.
SMA – Ideal	7.48	2.91	6.13	2.94	3.41	2.59
RT – Ideal	7.48	2.89	4.37	2.75	5.35	3.00
SMA – Real	9.95	7.89	8.40	7.56	3.82	4.36
RT – Real	7.84	3.28	5.03	3.54	5.02	3.06
WLS	29.32	8.23	13.13	7.27	23.85	11.60

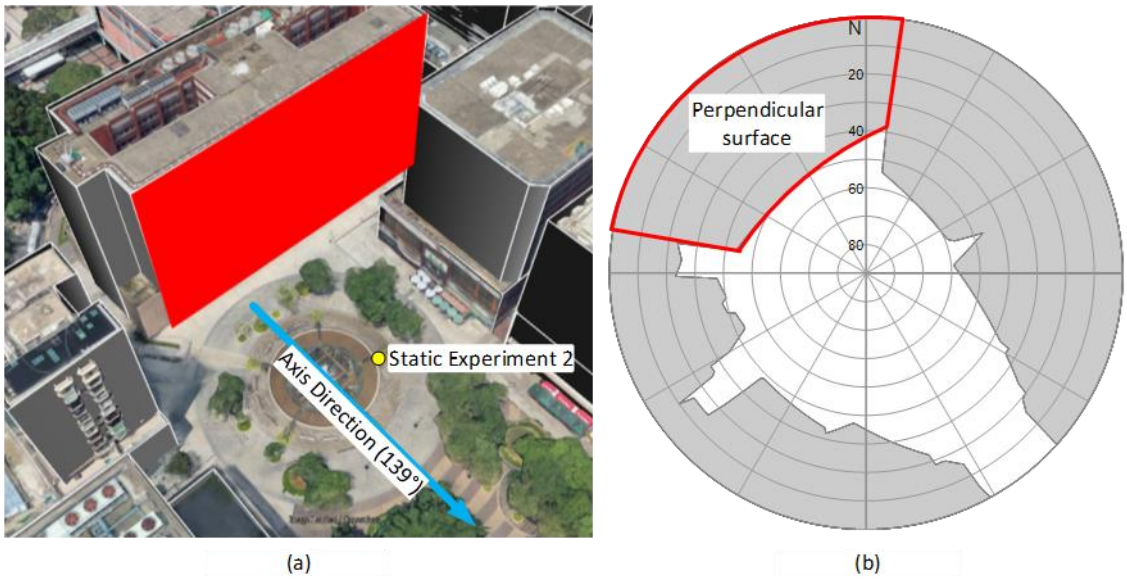

Figure 10 - Static experiment 2 environment (left) and the corresponding skymask (right)

In static experiment 2, the mean error of the skymask axis method of the ideal and real case are 7.48m and 9.95m respectively, compared to the ray-tracing algorithm of mean error are 7.48m and 7.84m. In Figure 9 can observe that, some solution of skymask align axis method real case results in a larger error in the along direction. This error is cause by the NLOS reflection that misdetection of the reflecting point by the skymask align axis due to the perpendicular surface. For the NLOS satellite that 'hide' behind that surface, e.g., the satellite that placed inside the red framed in Figure 10(b), the axis miss-detect the reflecting point exists, which results in labeled that signal is a valid one but provide an incorrect NLOS correction. This error contributes a large error for some position candidates and results in a large position result error.

The last static experiment was taken in the Tsuen Wan West, Hong Kong, as Figure 7(b). This place is more urban compare to the environment with above two static experiments.

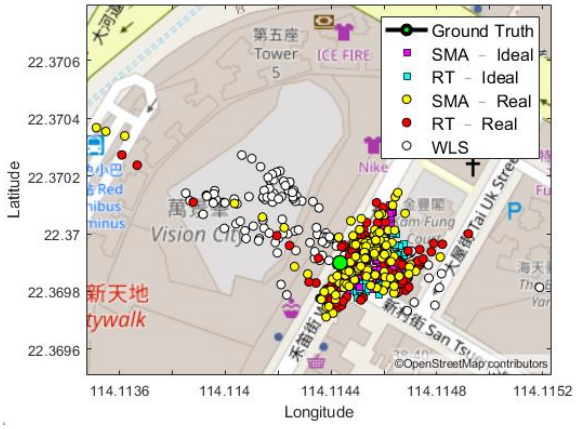

Figure 11 - Static experiment 3 results

Table 4 - Static experiment 3 (SMA: skymask axis method, RT: ray-tracing, WLS: weighted least square)

	2D-Error (m)		Along-Street Error (m)		Across-Street Error (m)	
	Mean	S.D.	Mean	S.D.	Mean	S.D.
SMA – Ideal	16.00	5.44	9.54	7.38	11.06	4.25
RT – Ideal	15.94	4.13	7.17	5.55	13.28	3.55
SMA – Real	18.27	15.75	10.18	7.46	12.13	16.62
RT – Real	17.12	14.09	9.77	6.56	11.55	14.82
WLS	29.95	16.02	8.48	5.87	27.92	16.38

This experiment is relative harsh that the street width is about 10m only with tall buildings standing at two sides of the street. Which the NLOS satellites account for about 60% of received satellites, and means the NLOS correction may need a more precise correction to achieve an acceptable solution accuracy. The skymask align axis achieve a mean error on the ideal and real case for 16m and 18.27m error while the error for ray-tracing is 15.94m and 17.12m respectively. The proposed skymask axis method can still achieve a similar accuracy with ray-tracing.

5. CONCLUSIONS AND FUTURE WORK

This paper proposes a novel algorithm that uses the building boundaries on skyplot, also called skymask, to correct the possible reflecting point for NLOS signal to simulated pseudorange for a scoring scheme based on comparing the similarity between position candidates. Comparing with the ray-tracing, using the skymask to provide the NLOS delay correction requires lower computation power and time-consuming with no extra equipment is required, so that this approach is practically applicable in portable devices. Wherever the skymask of that place is available, the algorithm can provide the NLOS delay correction for simulated pseudorange. The similarity between the measurements and simulated pseudorange with NLOS correction is then regarded as the confidence of the position candidate.

In the near future, the skymask align axis should be estimated by a more efficient way to determine the direction of the align axis in real time or in an offline process. This can increase the accuracy on determine the possible reflecting point on the skymask and result in a more accurate NLOS correction. Furthermore, benefits from the computation load reduction, the algorithm may able to develop more advance to consider multiple reflections of the signal path to enhance the NLOS correction accuracy, especially those NLOS labeled signal with no reflection found.

REFERENCES

1. Hsu, L.-T., *Analysis and modeling GPS NLOS effect in highly urbanized area*, in *GPS Solutions*. 2018. p. 7.
2. Groves, P.D. and Z. Jiang, *Height Aiding, C/N0 Weighting and Consistency Checking for GNSS NLOS and Multipath Mitigation in Urban Areas.* Journal of Navigation, 2013. **66**(5): p. 653-669.
3. Hsu, L., et al., *Multiple Faulty GNSS Measurement Exclusion Based on Consistency Check in Urban Canyons.* IEEE Sensors Journal, 2017. **17**(6): p. 1909-1917.

4. Jiang, Z. and P.D. Groves, *NLOS GPS signal detection using a dual-polarisation antenna.* GPS Solutions, 2014. **18**(1): p. 15-26.
5. Wen, W., G. Zhang, and L.-T. Hsu, *Correcting GNSS NLOS by 3D LiDAR and Building Height*. Proceedings of the 31st International Technical Meeting of The Satellite Division of the Institute of Navigation (ION GNSS+ 2018). 2018, Miami, Florida. 3156-3168.
6. Moreau, J., S. Ambellouis, and Y. Ruichek, *Fisheye-Based Method for GPS Localization Improvement in Unknown Semi-Obstructed Areas.* Sensors, 2017. **17**(1): p. 119.
7. Suzuki, T. and N. Kubo, *N-LOS GNSS signal detection using fish-eye camera for vehicle navigation in urban environments*. Vol. 3. 2014. 1897-1906.
8. Wang, L., P.D. Groves, and M.K. Ziebart, *GNSS Shadow Matching: Improving Urban Positioning Accuracy Using a 3D City Model with Optimized Visibility Scoring Scheme*, in *Navigation*. 2013. p. 195-207.
9. Groves, P., *Shadow Matching: A New GNSS Positioning Technique for Urban Canyons*. Vol. 64. 2011. 417-430.
10. Miura, S., L.-T. Hsu, and F. Chen, *GPS Error Correction With Pseudorange Evaluation Using Three-Dimensional Maps*, in *IEEE Transactions on Intelligent Transportation Systems*. 2015. p. 3104-3115.
11. Hsu, L.-T., Y. Hu, and S. Kamijo, *3D building model-based pedestrian positioning method using GPS/GLONASS/QZSS and its reliability calculation*, in *GPS Solutions*. 2016. p. 413-428.
12. Adjrad, M. and P.D. Groves, *Intelligent Urban Positioning: Integration of Shadow Matching with 3D-Mapping-Aided GNSS Ranging.* Journal of Navigation, 2018. **71**(1): p. 1-20.
13. Ziedan, N.I., *Urban Positioning Accuracy Enhancement Utilizing 3D Buildings Model and Accelerated Ray Tracing Algorithm*. Proceedings of the 30th International Technical Meeting of The Satellite Division of the Institute of Navigation (ION GNSS+ 2017). September 2017, Portland, Oregon. pp. 3253 - 3268.
14. Realini, E. and M. Reguzzoni, *Gogps: open source software for enhancing the accuracy of low-cost receivers by single-frequency relative kinematic positioning.* goGPS: open source software for enhancing the accuracy of low-cost receivers by single-frequency relative kinematic positioning, 2013. **24**(11): p. 115010.
15. Groves, P.D. and M. Adjrad, *Multi-Epoch 3D Mapping Aided GNSS using a Grid Filter*. Proceedings of the 31st International Technical Meeting of The Satellite Division of the Institute of Navigation (ION GNSS+ 2018). September 2018, Miami, Florida. pp. 3335-3356.
16. *Explanatory Notes on Geodetic Datums in Hong Kong*, L.D. Survey and Mapping Office, Editor. 1995: Hong Kong Special Administrative Region.